Suppression of murine cerebral F_2-isoprostanes and F_4-neuroprostanes from excitotoxicity and innate immune response in vivo by α- or γ-tocopherol

Dejan Milatovic, Mike VanRollins, Ke Li, Kathleen S. Montine, Thomas J. Montine *

Department of Pathology, University of Washington, Harborview Medical Center, Box 359791, Seattle, WA 98104, USA

Abstract

Oxidative damage to brain is a featured shared by several destructive and degenerative diseases and is thought to contribute to disease pathogenesis. Two commonly proposed sources of the increased free radical stress that leads to oxidative damage in several of these diseases are excitotoxicity and activation of innate immunity, both of which are proposed pharmacologic targets. Here we used models of excitotoxicity, intracerebroventricular (ICV) kainate (KA), and innate immune activation, ICV lipopolysaccharide (LPS), to test the effectiveness of peripherally administered α-tocopherol (AT) and γ-tocopherol (GT) as neuroprotectants. We quantified murine cerebral oxidative damage by measuring F_2-isoprostanes (IsoPs) and F_4-neuroprostanes (NeuroPs) using stable isotope dilution methods followed by gas chromatography–mass spectrometry with selective ion monitoring. Our data showed that peripherally administered AT and GT were equally effective at suppressing acute oxidative damage from direct excitotoxicity caused by KA. In contrast, peripherally administered AT, but not GT, was effective at suppressing delayed neuronal oxidative damage from activated glial innate immune response. These data imply that AT may be more broadly protective of cerebrum from oxidative damage in different disease contexts.
© 2005 Elsevier B.V. All rights reserved.

Keywords: Brain; Oxidative damage; Tocopherol; Isoprostane; Neuroprostane

1. Introduction

Oxidative damage to brain is a featured shared by many destructive and degenerative diseases [1,2]. The sources of increased free radical stress in these diseases are varied with some being shared among several diseases while others are disease-specific. An example of the latter is amyloid β (Aβ), which is proposed to play a direct role in generating free radical stress in Alzheimer's disease (AD) [3]. Two examples of the former are excitotoxicity and activation of innate immunity [4]. Diseases of brain associated with increased innate immune response include AD, Parkinson's disease (PD), HIV-associated dementia (HAD), ischemia, head trauma, cerebral palsy, axonal degeneration in multiple sclerosis, and perhaps even autism [5,6]. Diseases of brain associated with

excitotoxicity include virtually all of these plus others, e.g. Huntington's disease and epilepsy [7,8].

Glial innate immune response can be activated by a single intracerebroventricular (ICV) injection of lipopolysaccharide (LPS), a major component of Gram negative bacterial cell walls. We have shown previously that this LPS-activated glial innate immune response leads to indirect neuronal oxidative damage and synaptodendritic degeneration exclusively through a CD14-dependent mechanism free of behavioral or febrile response, and that LPS itself has no direct toxic effect on neurons [9,10]. It is noteworthy that although the molecular determinants of this signaling cascade were initially discovered in pursuit of microorganism-mediated innate immune response, it is now appreciated that CD14-dependent signaling also is activated by endogenous ligands. For example, CD14-dependent activation is a component of the cellular response to Aβ fibrils and to neoantigens expressed by apoptotic cells [11–14].

* Corresponding author. Tel.: +1 206 341 5248.
E-mail address: tmontine@u.washington.edu (T.J. Montine).

Excitotoxicity can be stimulated by ICV injection of kainic acid (KA), the active ingredient originally isolated from seaweed used as an herbal treatment for ascariasis [15]. Kainate is a rigid analog of glutamate, the principal excitatory neurotransmitter in CNS, and is a very potent stimulant of a subset of ligand-gated ion channels called KA receptors [16]. It is important to stress that KA has profound direct effects on neurons with little direct effect on glia. However, at later stages of KA toxicity, glial response to damaged and dying neurons does occur. In this respect, the early response to KA is a classical direct neurotoxic insult that is distinct from LPS which damages neurons indirectly via glial innate immune activation.

Several methods exist to determine free radical-mediated damage to cells. While most of these function well in vitro, important limitations arise in living systems where extensive, highly active enzymatic pathways have evolved to metabolize many of the commonly measured products, such as 4-hydroxynonenal [17]. One method that has been extensively replicated as a robust means of quantifying free radical damage in vivo is measurement of F_2-isoprostanes (F_2-IsoPs) [18], a group of prostanoid isomers generated from free radical damage to arachidonic acid (AA) that are not extensively metabolized in situ. Since AA is present throughout brain and within different cell types in brain at roughly equal concentrations, measurement of cerebral F_2-IsoPs, like all other measures of oxidative damage, reflects damage to brain tissue but not necessarily to neurons. For these reasons, we developed an assay to measure the analogous products generated from docosohexaenoic acid (DHA), F_4-neuroprostanes (NeuroPs) [19]. Since DHA is highly concentrated in neuronal membranes, F_4-NeuroPs offer a unique window into free radical damage to neuronal membranes in vivo [20].

Several clinical studies have attempted either to associate dietary tocopherol consumption with the prevalence of AD or to treat AD with AT [21–23]. While the epidemiologic data have been encouraging [22,23], and some clinical trials have met with modest success [21], it is still unclear what dose or combination of tocopherol isomers is most effective at suppressing oxidative damage to cerebrum. Indeed, while there are several studies that investigated AT and GT in vitro, in cell culture, or in ex vivo preparations [24], we are unaware of any study that has directly compared their relative anti-oxidant efficacy in vivo with these models of cerebral oxidative damage. The studies presented here investigated the efficacy of AT and GT in suppressing the accumulation of F_2-IsoPs and F_4-NeuroPs, in murine cerebrum following excitotoxic insult or activation of innate immune response.

2. Experimental

The University of Washington Institutional Animal Care and Use Committee approved all experiments. Male C57Bl/6J mice 5–8 weeks of age were used. Mice were housed at $21 \pm 1\,^{\circ}$C; humidity, $50 \pm 10\%$; and light/dark cy-cle, 12 h/12 h and had free access to pelleted food (Rodent Laboratory Chow, Purina Mills Inc., St. Louis, MO) and water. Following anesthesia, 5 µl intracerebroventricular (ICV) injections were delivered over 1 min into the left lateral ventricle using a 26 gauge Hamilton syringe and the external landmarks of 4 mm lateral to midline and 5 mm posterior from the forward edge of the left ear. Depth of injection was maintained at 3 mm by using a stylet. LPS (CalBiochem, San Diego, CA) was dissolved in phosphate buffered saline (pH 7.4) at a final concentration of 1 mg/ml for a total ICV dose of 5 µg. KA (Sigma Chemical Co., St. Louis, MO) was delivered by exactly the same method but with a total ICV dose of 1 nmol. AT and GT were dissolved in mineral oil and administered intraperitoneally (i.p.) in three doses on days -2, -1 and 0 relative to ICV injection. Mice were euthanized at the times indicated, their brains rapidly removed, the cerebral hemispheres dissected, flash frozen in liquid nitrogen, and stored at $-80\,^{\circ}$C.

Total lipids were extracted from mouse cerebrum using a modified Folch procedure. Frozen samples (0.1–0.5 g) were suspended in ice-cold 5 ml $CHCl_3$:CH_3OH (2:1, v/v), and homogenized 20 s (Polytron, Brinkmann Instruments, Westbury, NY); the generator was rinsed in 5 ml $CHCl_3$:CH_3OH (2:1). All solvents used were HPLC grade, and contained 0.005% (w/v) β-hydroxytoluene (BHT) to suppress oxidation. Aqueous solutions were prepared using freshly deionized H_2O. Extracts and rinses were combined, covered with a nitrogen blanket, and mixed every 10 min over 30 min at 25 °C. The lipid extracts were mixed vigorously with 2.0 ml NaCl (0.9%, w/v), and the phases separated by centrifugation at $300 \times g$ for 10 min at 25 °C. After the upper phase was decanted, samples were transferred to virgin tubes, and residual organic solvent was removed under a nitrogen stream. Total lipids were dissolved in 0.5 ml CH_3OH and stored at $-80\,^{\circ}$C.

Lipid extracts were saponified to release esterified prostanes. KOH (2.7N) in 0.5 ml water was added to lipid extracts in 0.5 ml CH_3OH. The mixture was sonicated and mixed vigorously until thoroughly suspended, and heated at 37 °C for 30 min. The pH was adjusted to 3.0 using ∼1.2 ml 1.0N HCl. Next, stable isotope-labeled analogs were added as internal standards: 500–1000 pg each of $[^2H_4$-3,3,4,4]-8-iso-$PGF_{2\alpha}$ (iso-$PGF_{2\alpha}$-III, Cayman Chemicals, Ann Arbor, MI) and $[^{18}O_2]17$-F_{4c}-NeuroP (generous gift from Dr. Jason Morrow, Vanderbilt University) were added to the neutralized prostanes.

Prostanes were isolated using reversed-phase and normal-phase solid-phase extractions (SPE). For reverse phase, Sep Pak Plus C18 columns (Waters Corp, Milford, MA) were wet with 5 ml CH_3OH (flow rate, ∼1.0 ml/min) and conditioned with 7.0 ml H_2O (adjusted to pH 3.0 with 1.0N HCl). With flow rates ∼0.5 ml/min, columns were charged with sample, then washed with 10 ml H_2O (pH 3.0) and 10.0 ml n-heptane. Prostanes were eluted in 10 ml n-heptane:ethyl acetate (1:1, v/v). For normal-phase SPE, Sep Pak Plus Silica (Waters) columns were used with a flow rate of ∼0.5 ml/min through-

out. Silica columns were conditioned with 5.0 ml ethyl acetate. Samples were mixed briefly with minimal amount of granular Na_2SO_4 to remove residual H_2O and immediately decanted into a syringe for application to a silica column. The charged column was washed with 5.0 ml ethyl acetate:*n*-heptane (3:1, v/v), and prostanes were eluted with 5.0 ml ethyl acetate:methanol (1:1, v/v).

Prostanes isolated by SPE were dried at 37 °C under a nitrogen stream, and derivatized to pentafluorbenzyl esters. Samples were vigorously mixed with 40 μl pentafluoroben-zyl bromide:anhydrous acetonitrile (10:90, v:v) plus 20 μl di-isopropylethylamine:acetonitrile (10:90, v:v). Following reaction at 37 °C for 20 min, the esters were dried under a nitrogen stream, and dissolved in 50 μl $CHCl_3$:CH_3OH (2:3, v:v). Next, TLC was performed to remove excess reagent. TLC was done using 5 cm × 20 cm glass plates covered with a 250 um layer of silica gel particles 60 Å in diameter (Partisil LK6D; Whatman, Maidstone, England). Just before use, plates were washed with ethyl acetate:ethanol (90:10), ac-

tivated at 95 °C for 20 min, and cooled in a dessicator. A TLC chamber was lined with filter paper and conditioned 30 min with 100 ml $CHCl_3$:CH_3CH_2OH (90:10, v:v). Samples (50 μl) were applied to the upper half of pre-adsorbent in four pre-scored lanes, and dried 5–10 s with a hair dryer. Sample plates were added to both ends of the chamber. In contrast, TLC standard (5 μg/5 μl CH_3OH) was applied to a separate plate that was positioned towards the center of the TLC chamber. After the chamber was rapidly closed, solvent was allowed to migrate 15 cm, and the plates removed. Sample Rfs were calculated from standards visualized by spraying with phosphomolybdic acid (Sigma Chemical Co., St. Louis, MO) and heating. Samples were outlined, scraped onto weighing paper, transferred to 1.7 ml microfuge tubes (ISC BioExpress, Kayville, UT), and mixed vigorously with 1.0 ml ethyl acetate. Following centrifugation at $16,000 \times g$ for 8 min at 4 °C, prostane pentafluorobenzyl esters were transferred in the ethyl acetate to a virgin microfuge tube and stored at −80 °C.
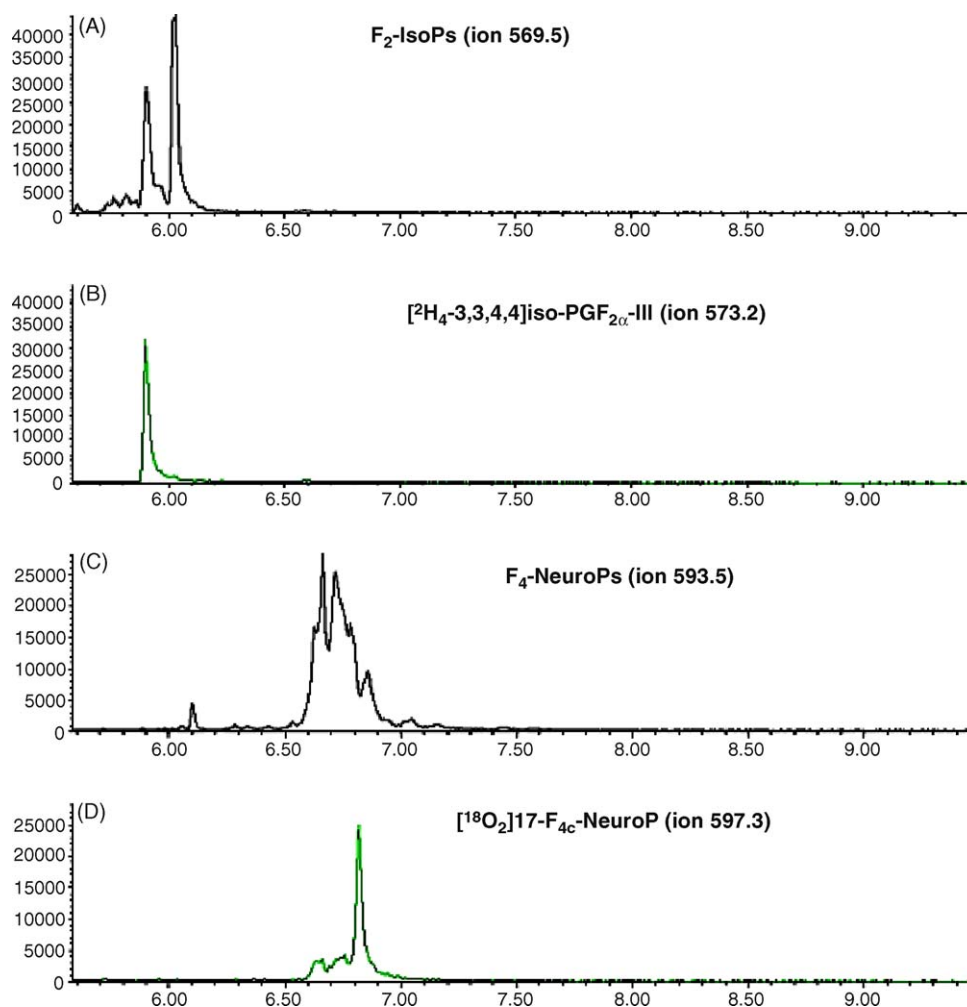

Fig. 1. Chromatograms for F_2-IsoPs and F_4-NeuroPs from mouse cerebrum. All chromatograms plot abundance vs. time (min). (A) *m/z* 569.5 chromatogram showing F_2-IsoPs, (B) *m/z* 573.2 chromatogram showing F_2-IsoP internal standard, (C) *m/z* 593.5 chromatogram showing F_4-NeuroPs, and (D) *m/z* 597.3 chromatogram showing F_4-NeuroP internal standard.

Just prior to GC/MS analysis, labile hydroxyl groups of prostanes were converted to heat-stable silylethers. After being dried under a nitrogen stream, samples were dissolved in 8 μl dimethylformamide, mixed with 20 μl bis(trimethylsilyl)trifluoroacetamide (Pierce Chemical Co., Rockford, IL), and heated 5.0 min at 37 °C. Silylated samples were dried at 37 °C under a nitrogen stream, suspended in 23 μl undecane, and transferred into 250 μl glass inserts on plastic springs (#680843-629, Kimble Glass, Vineland, NJ).

Prostanes were resolved by a 6890N gas-chromatographic system fitted with a 7683 Series automatic liquid sampler, 10 μl Hamilton syringe, and split/splitless injector (Agilent Technologies, Palo Alto, CA). Just prior to being subjected to a pulse of helium (18 psig, 30 s), samples (2 μl) were injected into a 900 μl single "gooseneck" glass insert (265 °C), and developed on a 25 m × 0.25 mm capillary column; the last 15 m of capillary wall was coated (0.25 μm) with polar phase ((14%-cyanopropylphenyl)methylpolysiloxane; DB-1701, Agilent Technologies). Using BIP quality helium (Air Products, Puyallup, WA), flow was maintained at a constant linear velocity of 54 cm/s; 1.0 min after injection, column temperature was programmed to rise from 200 to 300 °C at a rate of 20 °C/min. The transfer line into the ion source was 300 °C.

Endogenous prostanes levels were measured using isotope-dilution techniques and a quadrupole mass spectrometer (Model 5973, Agilent Technologies) in the negative-ion chemical ionization mode. Pressure of the reagent gas (CH_4) was set to 38 Torr, while the ion source and rods were kept at 200 °C. Four ions were monitored, each with a dwell time of 50 ms. Areas under peaks for m/z 569.5 and 573.2 (internal standard) plus m/z 593.5 plus 597.3 (internal standard), were manually integrated to quantify IsoP and NeuroP concentrations, respectively (Fig. 1). The coefficient of variance for both assays is less than 8%.

3. Results

ICV injection of the amount of LPS used in these experiments leads to reactive morphologic features of microglia and astrocytes, but does not recruit an adaptive immune response in brain until several days after injection, and does not lead to behavioral changes or a febrile response [25,26]. Similarly, while mice entered status epilepticus within a minute of ICV KA injection, KA-induced seizures do not lead to activated resident inflammatory cells in brain until several days (>4) after exposure, outside of the time frame used in these experiments [27].

Our first set of experiments compared the time course for cerebral oxidative damage following exposure to ICV LPS or ICV KA (Fig. 2). There was no change in cerebral F_2-IsoPs of F_4-NeuroPs over 24 h following ICV PBS vehicle; average (+S.D.) basal F_2-IsoPs = 3.2 + 0.3 ng/g and basal F_4-NeuroPs = 12.6 + 2.7 ng/g. There was a rapid onset of detectable oxidative damage with ICV KA that was greatest at
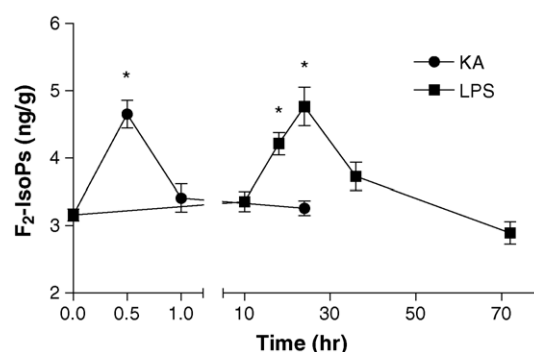

Fig. 2. Time course for cerebral oxidative damage following ICV injection of KA or LPS. Data are F_2-IsoPs expressed as ng per g of tissue following injection at time = 0 ($n \geq 5$ per time point). *$P < 0.01$ compared to untreated control.

our earliest time point (30 min) following injection, returned to baseline by 60 min, and remained at baseline levels 24 h after injection. In contrast, indirect neuronal damage with ICV LPS generated delayed cerebral oxidative damage with no significant increase in cerebral F_2-IsoPs even 10 h after injection. However, following this delay, cerebral oxidative damage peaked at about 24 h following ICV LPS and then decreased to near baseline levels by 36 h. An identical time course has been observed for F_4-NeuroPs following LPS [26].

Our next series of experiments determined the dose–response relationships for tocopherol-mediated suppression of cerebral oxidative damage from direct neuronal damage by ICV KA (Fig. 3). All measurements for these experiments were done 30 min after ICV KA injection. The increase in F_4-NeuroPs was greater than that for F_2-IsoPs, likely a reflection of the greater susceptibility of DHA than AA to oxidation and similar to what was observed
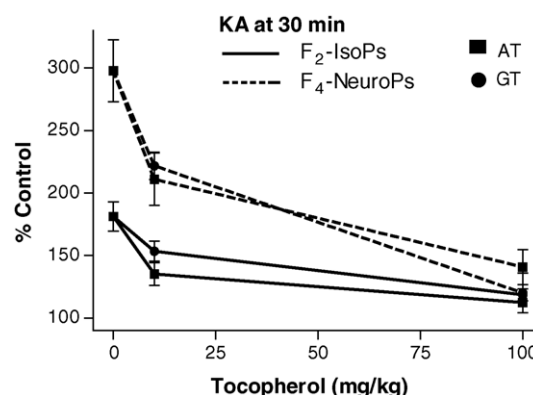

Fig. 3. Dose–response curves for tocopherol suppression of KA-induced cerebral oxidative damage. Peripheral (i.p.) administration of α- or γ-tocopherol (AT or GT) was made at days −2, −1 and 0 relative to ICV injection of KA; mice were sacrificed 30 min later. Data are expressed percent of control mice that received neither KA nor tocopherol ($n \geq 5$ for each group). Two-way ANOVA (tocopherol vs. dose) for F_2-IsoP or F_4-NeuroP data had $P < 0.0001$ for dose but $P > 0.05$ for AT vs. GT or interaction between terms.
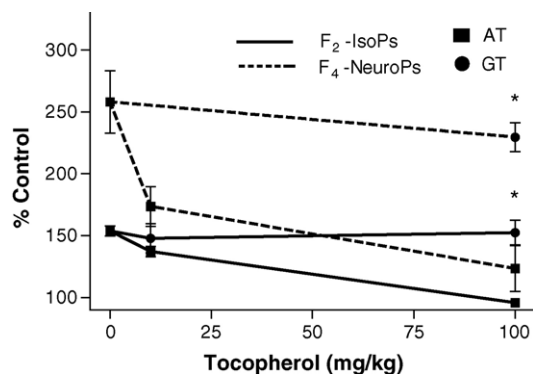
Fig. 4. Dose–response curves for tocopherol suppression of LPS-induced cerebral oxidative damage. Peripheral (i.p.) administration of α- or γ-tocopherol (AT or GT) was made at days −2, −1 and 0 relative to ICV injection of LPS; mice were sacrificed 24 h later. Data are expressed percent of control mice that received neither LPS nor tocopherol ($n \geq 5$ for each group). Two-way ANOVA (tocopherol vs. dose) for F_2-IsoP an F_4-NeuroP data had $P < 0.0001$ for dose, AT vs. GT, and interaction between terms. Bonferroni corrected posttests showed that AT and GT were significantly different ($^*P < 0.01$) at their highest dose for F_2-IsoPs and F_4-NeuroPs.

with LPS. AT and GT both partially but significantly and equivalently suppressed F_2-IsoP and F_4-NeuroP formation at 10 mg/kg. Similarly, at 100 mg/kg, both AT and GT nearly completely suppressed ICV KA-induced oxidative damage to cerebral AA and DHA; again, there were no significant differences between AT and GT.

We followed the same experimental protocol for tocopherol suppression of ICV LPS-induced cerebral oxidative damage, except now data were collected 24 h post injection (Fig. 4). As with suppression of oxidative damage from KA exposure, AT partially blocked F_2-IsoP and F_4-NeuroP formation at 10 mg/kg and nearly completely suppressed cerebral oxidation damage at 100 mg/kg. In sharp contrast to KA toxicity, however, GT did not significantly suppress LPS-induced oxidative damage even at 100 mg/kg.

4. Discussion

Here, we explored the capacity of peripherally administered tocopherols to suppress two distinct mechanisms of cerebral oxidative damage that have been implicated, at least as partial contributors, in a number of degenerative and destructive lesions of brain: innate immune activation by LPS and excitotoxicity by KA. We measured two markers of free radical damage to lipids, F_2-IsoPs and F_4-NeuroPs; the former reflecting oxidative damage to all cerebral tissue elements and the latter providing a relatively selective window into peroxidation of neuronal membranes. Our results showed that cerebral oxidative damage from these two toxins followed very different temporal profiles. KA led to the rapid onset of cerebral oxidative damage while LPS led to delayed oxidative damage. In both instances, the magnitude of cerebral oxidative damage achieved in these two models

was equivalent and comparable to that observed in diseased regions of brain from patients with AD [28].

Suppression of cerebral oxidative damage is an important goal in the treatment of neurological diseases, yet very little information exists on which compounds are most effective in the different contexts of disease-related oxidative damage to cerebrum, nor is there clear information on the doses necessary to protect brain. The lower concentration of tocopherols used here achieves plasma levels comparable to those observed in individuals taking dietary supplements [29] and the higher concentration likely approximates levels in clinical trials that used very large does of AT [21]. Although there are limitations in extrapolating from rodent models to humans, our data indicate that AT and GT partially overlap in their effectiveness as neuroprotectants from oxidative damage and that their effectiveness is at least partially related to the context of increased free radical stress. Specifically, we observed that peripheral administration of AT and GT were equivalent in protecting cerebrum from centrally administered KA. This was somewhat surprising because others have shown that AT more efficiently accumulates in the CNS following peripheral administration in rodents [30]. In addition, while AT and GT both terminate lipid peroxidation, AT is more potent than GT in this regard in a variety of in vitro and in vivo assays [24]. We speculate that this action accounts for the broad protective effect observed with AT. However, among its other actions, GT scavenges electrophiles such as peroxynitrite, an action that is not shared by AT [31]. Presumably this or some other specific action of GT accounts for its unexpectedly potent suppression of KA-induced cerebral oxidative damage. Similarly, since GT was ineffective in suppressing cerebral oxidative damage from LPS, we speculate that peroxynitrite and other reactive species scavenged by GT are not significantly contributing to oxidative damage in this model.

Unlike KA that directly damages neurons through the activation of ligand-gated ion channels, LPS is indirectly toxic to neurons through the activation of CD14/Toll-like receptor-4 on microglia [32]. This activation of microglia leads to increased expression of many genes, several of which are capable of producing free radical stress. This requirement for gene expression following ICV LPS is not an element of KA-induced toxicity and likely accounts, at least in part, for the delayed increase in cerebral oxidative damage observed with LPS but not KA. In contrast to our experiments with KA, GT was ineffective at suppressing LPS-induced oxidative damage.

In summary, our data demonstrated that peripherally administered AT and GT were equally effective at suppressing oxidative damage from direct excitotoxicity to neurons caused by KA. In contrast, peripherally administered AT, but not GT, was effective at suppressing neuronal oxidative damage from activated glial innate immune response. Further, these data imply that, of these two tocopherols, AT may be broadly protective of cerebrum from oxidative damage in different disease contexts.

Acknowledgements

References

[1] Y. Gilgun-Sherki, Z. Rosenbaum, E. Melamed, D. Offen, Pharmacol. Rev. 54 (2002) 271.

[2] B. Halliwell, Drugs Aging 18 (2001) 685.

[3] D.A. Butterfield, J. Drake, C. Pocernich, A. Castegna, Trends Mol. Med. 7 (2001) 548.

[4] T.J. Montine, D.G. Graham, in: D.I. Graham, P. Lantos (Eds.), Greenfield's Neuropathology, Arnold, London, 2002, p. 799.

[5] E. Polazzi, A. Contestabile, Rev. Neurosci. 13 (2002) 221.

[6] D.L. Vargas, C. Nascimbene, C. Krishnan, A.W. Zimmerman, C.A. Pardo, Ann. Neurol. 57 (2005) 67.

[7] M.N. Patel, Free Radic. Res. 36 (2002) 1139.

[8] T. Grunewald, M.F. Beal, Ann. N. Y. Acad. Sci. 893 (1999) 203.

[9] T.J. Montine, D. Milatovic, R.C. Gupta, T. Valyi-Nagy, J.D. Morrow, R.M. Breyer, J. Neurochem. 83 (2002) 463.

[10] S. Zaja-Milatovic, D. Milatovic, A.M. Schantz, J. Zhang, K.S. Montine, A. Samii, A.Y. Deutch, T.J. Montine, Neurology 64 (2005) 545.

[11] J.L. Imler, J.A. Hoffmann, Trends Cell Biol. 11 (2001) 304.

[12] S. Akira, J. Biol. Chem. 278 (2003) 38105.

[13] K. Fassbender, S. Walter, S. Kuhl, R. Landmann, K. Ishii, T. Bertsch, A.K. Stalder, F. Muehlhauser, Y. Liu, A.J. Ulmer, S. Rivest, A. Lentschat, E. Gulbins, M. Jucker, M. Staufenbiel, K. Brechtel, J. Walter, G. Multhaup, B. Penke, Y. Adachi, T. Hartmann, K. Beyreuther, FASEB J. 18 (2004) 203.

[14] O.D. Moffatt, A. Devitt, E.D. Bell, D.L. Simmons, C.D. Gregory, J. Immunol. 162 (1999) 6800.

[15] D.C. Anthony, T.J. Montine, D.G. Graham, in: C.D. Klaasen (Ed.), Casarett and Doull's Toxicology: The Basic Science of Poisons, McGraw-Hill, New York, 2001, p. 535.

[16] J.E. Huettner, Prog. Neurobiol. 70 (2003) 387.

[17] T.J. Montine, M.D. Neely, J.F. Quinn, M.F. Beal, W.R. Markesbery, L.J. Roberts II, J.D. Morrow, Free Radic. Biol. Med. 33 (2002) 620.

[18] J.D. Morrow, L.J. Roberts, Prog. Lipid Res. 36 (1997) 1.

[19] L.J. Roberts II, T.J. Montine, W.R. Markesbery, A.R. Tapper, P. Hardy, S. Chemtob, W.D. Dettbarn, J.D. Morrow, J. Biol. Chem. 273 (1998) 13605.

[20] K.S. Montine, J.F. Quinn, J. Zhang, J.P. Fessel, L.J. Roberts II, J.D. Morrow, T.J. Montine, Chem. Phys. Lipids 128 (2004) 117.

[21] M. Sano, C. Ernesto, R.G. Thomas, M.R. Klauber, K. Schafer, M. Grundman, P. Woodbury, J. Growdon, C.W. Cotman, E. Pfeiffer, L.S. Schneider, L.J. Thal, N. Engl. J. Med. 336 (1997) 1216.

[22] M.C. Morris, D.A. Evans, J.L. Bienias, C.C. Tangney, D.A. Bennett, N. Aggarwal, R.S. Wilson, P.A. Scherr, JAMA 287 (2002) 3230.

[23] M.J. Engelhart, M.I. Geerlings, A. Ruitenberg, J.C. van Swieten, A. Hofman, J.C. Witteman, M.M. Breteler, JAMA 287 (2002) 3223.

[24] R. Brigelius-Flohe, M.G. Traber, FASEB J. 13 (1999) 1145.

[25] C. Montero-Menie, L. Sindji, A. Pouplard, F. Jehan, L. Denechaud, F. Darcy, Brain Res. 653 (1994) 101.

[26] D. Milatovic, S. Zaja-Milatovic, K.S. Montine, P.J. Horner, T.J. Montine, J. Neurochem. 87 (2003) 1518.

[27] M. Lerner-Natoli, P. Montpied, M.C. Rousset, J. Bockaert, G. Rondouin, Epilepsy Res. 41 (2000) 141.

[28] E.E. Reich, W.R. Markesbery, L.J. Roberts II, L.L. Swift, J.D. Morrow, T. Montine, Am. J. Pathol. 158 (2001) 293.

[29] I. Jialal, M. Traber, S. Devaraj, Curr. Opin. Lipidol. 12 (2001) 49.

[30] M. Clement, L. Dinh, J.M. Bourre, Biochim. Biophys. Acta 1256 (1995) 175.

[31] S. Christen, A.A. Woodall, M.K. Shigenaga, P.T. Southwell-Keely, M.W. Duncan, B.N. Ames, Proc. Natl. Acad. Sci. U.S.A. 94 (1997) 3217.

[32] S. Zaja-Milatovic, D. Milatovic, A.M. Schantz, J. Zhang, K.S. Montine, A. Samii, A.Y. Deutch, T.J. Montine, Neurology 64 (2005) 545.